Theoretical Studies of Radiative Properties of Broken Clouds

G. A. Titov
Institute of Atmospheric Optics
Russian Academy of Science
Tomsk, Russia

One of the three major goals of the Atmospheric Radiation Measurement (ARM) Program is to improve the quality of radiation models under clear sky, homogeneous cloud, and broken cloud conditions. This report is concerned with the development of the theory of radiation transfer in the broken clouds. Our approach is based on a stochastic description of the interaction between the radiation and cloud field with stochastic geometry; the main results are presented in Titov (1990, 1993). In the following, we discuss

- the mean radiation fluxes in the near IR spectral range 2.7 to 3.2 μm
- the influence of random geometry of individual cumulus clouds on the mean fluxes of visible solar radiation
- the equations of the mean radiance in the statistically inhomogeneous cloud fields.

Mean Radiation Fluxes in the 2.7 to 3.2 μm Wavelength Range

In radiation models, as components of general circulation models (GCMs), one should calculate very accurately the net fluxes of upwelling and downwelling radiation at chosen levels in the atmosphere. These fluxes can be calculated by integrating the spectral fluxes; and, in turn, in calculating latter characteristics, one should take accurately into account the wavelength dependences of optical parameters of clouds and aerosols and of the absorbing properties of atmospheric gases.

In the wavelength range 2.7 to 3.2 μm, the real and imaginary parts of the water refractive index and, hence, the single scattering albedo and scattering phase function are strong functions of wavelength (Figure 1).

To the extent that the single scattering albedo is small (~0.5-0.6), the mean spectral albedo will result mainly from the radiation having undergone only several first orders of scattering. For this reason, the mean spectral albedo will be strongly influenced by the scattering phase function. The use of only one scattering phase function for calculating the mean spectral albedo, which is the commonly used approximation, may lead to large errors (Figure 2).

The dependence of the mean spectral albedo on the wavelength and cloud type (cumulus or stratus) is shown in Figure 3. Calculations were performed both with and without regard to absorption by water vapor and carbon dioxide. In the presence of absorption by water droplets, the mean spectral albedo $\langle R_{Cu} \rangle$ of a cumulus cloud field is larger than the mean spectral albedo $\langle R_{St} \rangle$ for stratus clouds even at the zero solar zenith angles $\zeta_0°$; whereas, in the visible spectral range, where the scattering can be treated as conservative (for which the single scattering albedo is equal to 1), the opposite is true.

Figure 4 illustrates the dependence of the value of $\Delta R = \langle R_{St} \rangle - \langle R_{Cu} \rangle$ on the single scattering albedo W: for a certain value of W_o, the value of ΔR alters its sign. In interpreting this effect, one must keep in mind that the significant contributor to the mean spectral albedo of cumulus clouds field is that radiation exiting the sides of a large number of cumulus clouds undergoes, on the average, fewer scattering orders than the radiation exiting the tops and bottoms of stratus clouds. From this fact and from the possibility to represent the mean albedo in terms of scattering order series, it follows that the lower scattering orders will be more of a factor to the mean albedo of cumulus clouds than of stratus clouds; for higher scattering orders, the opposite may be valid. As the single scattering

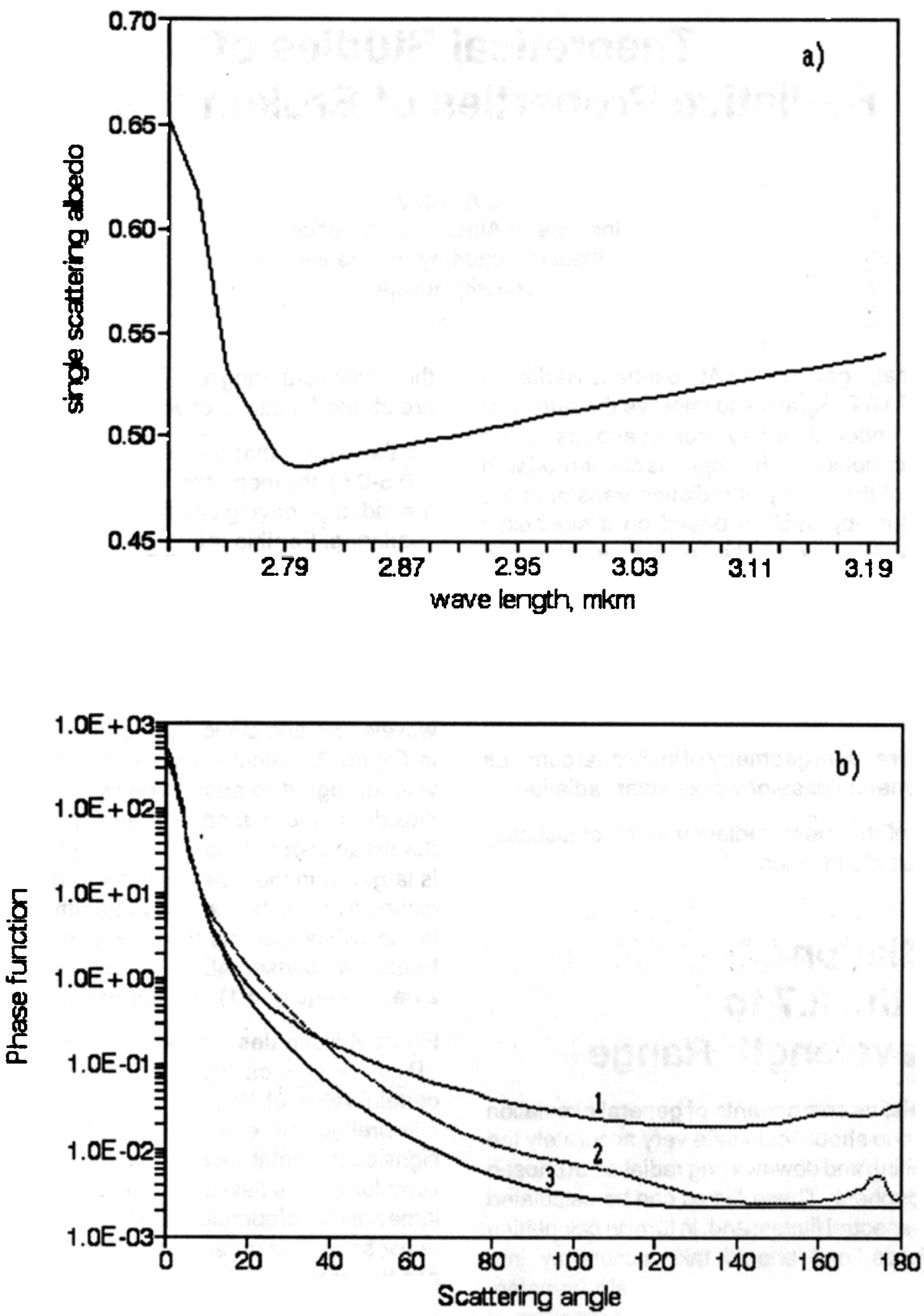

Figure 1. Single scattering albedo as a function of wavelength (a) and the phase functions for different wavelengths (b): $\lambda = 2.73$ μm (1); $\lambda = 2.79$ μm (2); $\lambda = 3.2$ μm (3).

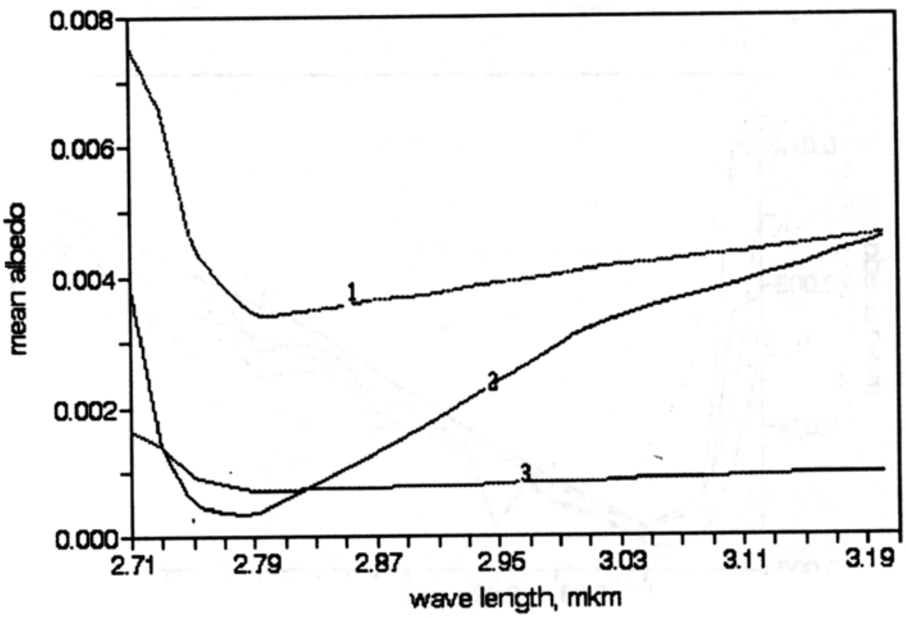

Figure 2. The influence of scattering phase functions $g_\lambda(\mu)$ on mean albedo where $\sigma = 30\ km^{-1}$; H = D = 0.5 km, N = 0.5, $\zeta_0 = 1°$: standard calculations (2); $\lambda = 2.73\ \mu m$ (3); $\lambda = 3.2\ \mu m$ (1).

albedo decreases, the relative role of high scattering orders becomes less important, which provides the explanation for the effect given in Figures 3 and 4.

Radiation Transfer in Statistically Inhomogeneous Cloud Fields

The equations for mean radiance were obtained in statistically homogeneous cloud fields (Titov 1990 and 1993). In reality, cloud cover is statistically inhomogeneous if, for no other reason, than the physically distinguishable vertical direction in the atmosphere. At present, numerical simulation of brightness and radiation fields (Titov 1990, 1993) is practically the only technique for calculating the mean fluxes and brightness fields of radiation modulated by statistically inhomogeneous broken clouds. In this method, one of the input parameters is the cloud shape, which is difficult to determine experimentally and to describe accurately by mathematical facilities, especially considering the highly irregular and "wild" shapes of real clouds.

For model calculations, individual clouds are approximated by truncated paraboloids of rotation. The cloud is divided into *m* layers and in each layer the true cloud shape is approximated by a cylinder. This approximation can be made with as high a resolution as desirable. The unconditional and conditional probabilities of cloud occurrence are specified as constant functions and within each layer the cloud field is statistically homogeneous. As a result, in each layer the equations for mean radiance hold with the corresponding changes in boundary conditions. The final result can be easily obtained if one successively uses the equations for mean radiance with the corresponding unconditional and conditional probabilities of cloud occurrence.

Presented in Table 1 are the mean fluxes of direct $\langle S \rangle$ and diffuse $\langle Q_S \rangle$ transmitted radiations, as well as the mean albedo $\langle R \rangle$ calculated with the method of numerical simulation (MNS) and with the equations for mean radiance (EMR). As the table shows, the calculational results are in good agreement.

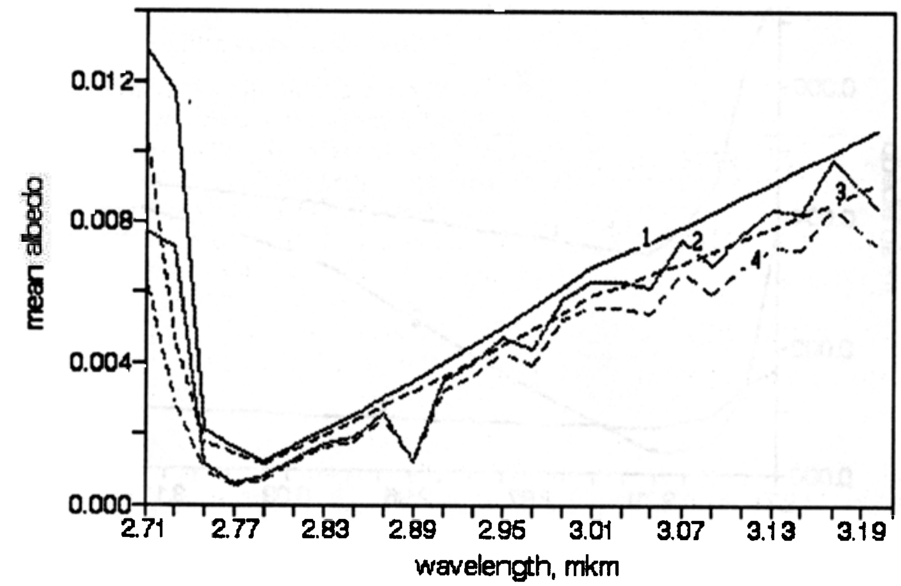

Figure 3. The mean albedos with $\sigma = 30\ km^{-1}$, H = D = 0.5 km, N = 0.5, $\zeta_o = 0°$ for different cloud types: Cu, without taking the gas absorption into account (1); Cu, taking into account the absorption by water vapor (2); St, without taking the gas absorption into account (3); St, taking into account the absorption by water vapor (4).

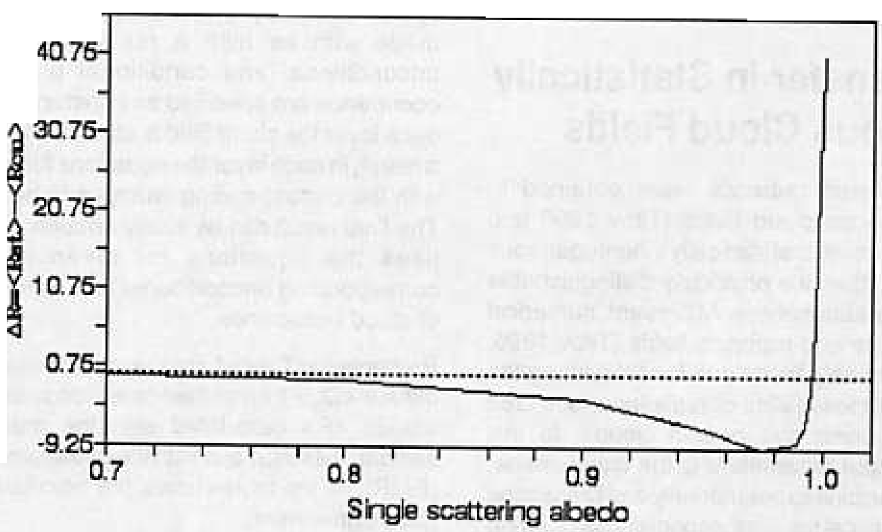

Figure 4. The influence of the single scattering albedo on the value of $\Delta R = \langle R_{St} \rangle - \langle R_{Cu} \rangle$ ($\Delta R * 10^3$) with $\zeta_o = 0°$, N = 0.5, surface albedo $A_S = 0$, $\gamma = H/D = 2$, $\tau = 60$.

Table 1. The mean fluxes calculated by two different methods with D = 1 km, $\sigma = 30\ km^{-1}$, H = 0.5 km, $\zeta_0 = 60°$

	<S>		$<Q_s>$		<R>	
N	MNS	ERM	MNS	ERM	MNS	ERM
0.10	0.878	0.857	0.069	0.086	0.053	0.053
0.30	0.629	0.615	0.199	0.218	0.171	0.168
0.50	0.419	0.404	0.316	0.324	0.265	0.272
0.70	0.211	0.213	0.389	0.395	0.401	0.392

The main advantages of the method, which is based on solving the equations for mean radiance, are as follows:

- Whereas in MNS the input parameter is the shape of individual clouds, in solving the EMR, the input parameters are the conditional and unconditional probabilities of cloud occurrence which have clear physical and mathematical meaning and can be determined experimentally.
- For intermediate and large cloud fractions the efficiency of the method based on EMR is much higher than that of the MNS.
- Equations for mean radiance can be solved not only with Monte Carlo techniques, but also with other numerical and approximate methods.

We hope that this approach to the problem of radiation transfer in statistically homogeneous cloud fields will be useful when the individual clouds have random geometry.

Models of Broken Clouds with Random Geometry of Individual Clouds

The models of broken cloudiness would be constructed by coupling the Poisson indicator field (P-model) and the sum of Gaussian fields (G_n-model) with decreasing variances and correlation radii (PG_n-model) (Babich and Titov 1992). This procedure is essentially very close to the generalized Brownian movement that is used to simulate fractal clouds.

The problem of numerical construction of sampling realizations in the PG_n-model is reduced to simulation of two types of independent random fields. The algorithms for simulating the Poisson indicator field and homogeneous isotropic Gaussian field with known spectral density can be found in Titov (1990, 1993) and Mikhailov (1978), while the basic idea of the algorithm is illustrated in Figure 5. The vertical cross sections of individual cumulus clouds in the PG_n-model are presented in Figure 6. As the figure shows, the obtained pictures are very close to realistic cloud images.

Figure 7 shows the mean fluxes of direct <S> and scattered transmitted $<Q_S>$ radiations, as well as the mean albedo <R>, which were calculated within appropriately coordinated P- and PG_1-models. The differences between the corresponding fluxes can reach essential magnitudes. The use of the PG_n models with n ~5-6 may result in random geometric cloud shapes that differ from the paraboloids (see Figures 5 and 6), and these differences may increase.

The results of comparison allows us to draw the preliminary conclusion that because of the nonlinear dependence of the radiation field upon the cloud characteristics, the random geometric shape of individual clouds can have a significant effect on the transfer of solar radiation.

References

Babich, E. A., and G. A. Titov. 1992. Mathematical Models of a Broken Cloud Field with a Random Geometry of Individual Clouds. *J. Atmos. Ocean. Optics.* **5**(7):757-765.

Mikhailov, G. A. 1978. *Dokl. Akad. Nauk SSSR*, **238**(4):793-795.

Titov, G. A. 1990. Statistical Description of Radiation Transfer in Clouds. *J. Atmos. Sci.* **47**(1):24-38.

Titov, G. A. 1993. Radiative Transfer in Cloud Field with Random Geometry. *Trends in Geophysical Researchs*, India (in press).

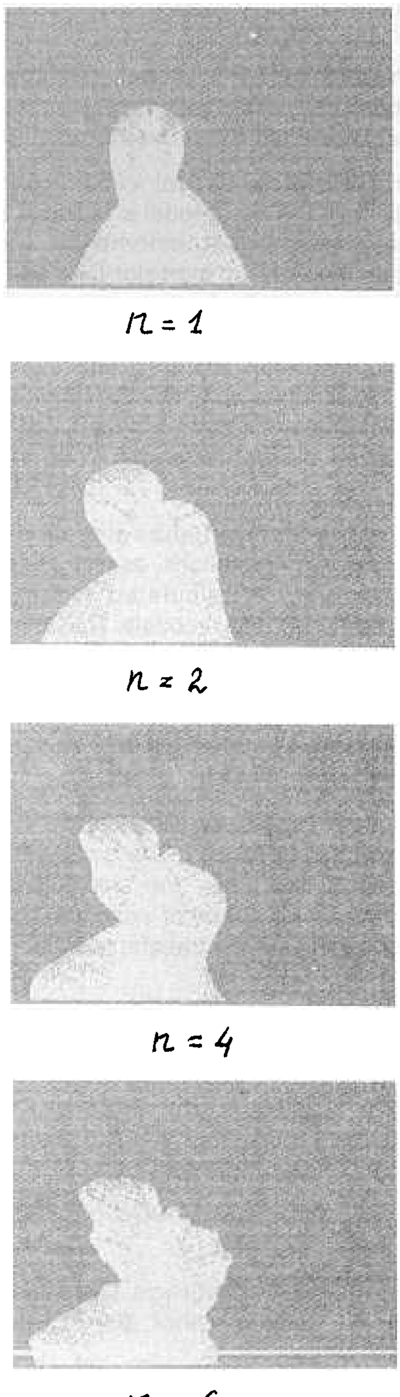

Figure 5. The basic idea of the algorithm for simulating the Poisson indicator field and homogeneous isotropic Gaussian field with known spectral density.

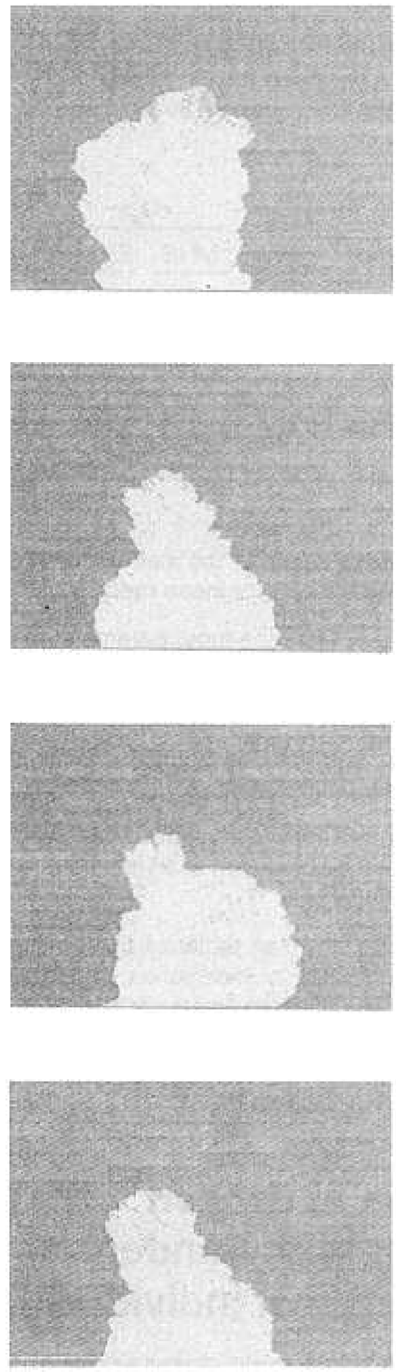

Figure 6. Vertical cross sections of individual cumulus clouds in the PG_n-model.

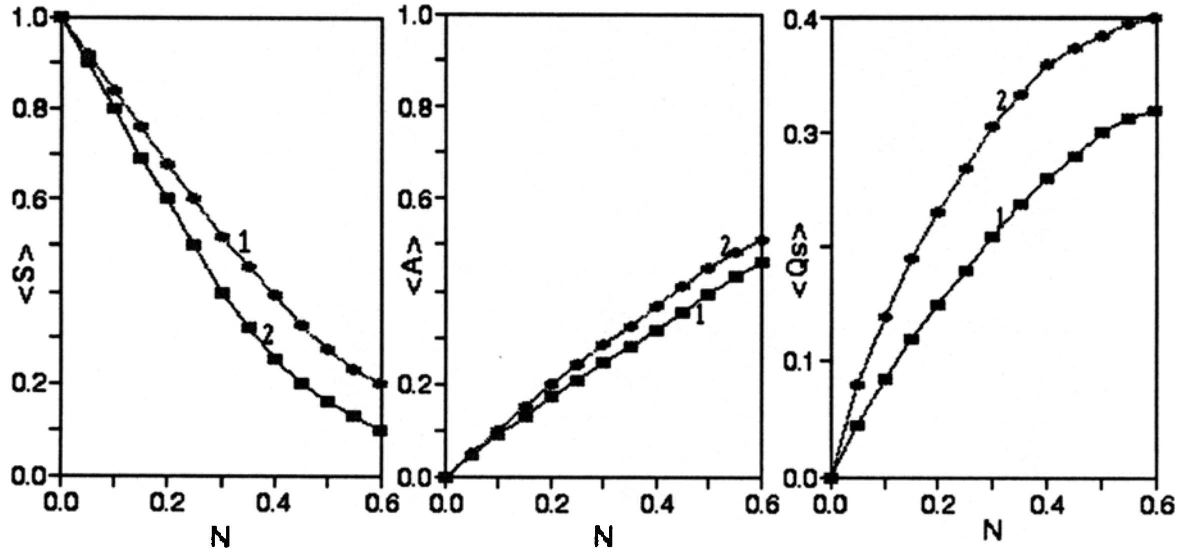

Figure 7. Dependence of the mean fluxes <S>, <A>, and $<Q_S>$ on the random geometry of individual clouds with ζ_o = 60°, σ = 30 km^{-1}, H = 1.06 km, and $<D^2>$ 1/2 = 1.143 km (curve 1 refers to the calculations for a P-model, curve 2 refers to PG_1-model).